Surface Chemistry

DOI: 10.1002/ange.201310776

Spatial and Directional Control over Self-Assembly Using Catalytic Micropatterned Surfaces**

Alexandre G. L. Olive, Nor Hakimin Abdullah, Iwona Ziemecka, Eduardo Mendes, Rienk Eelkema, and Jan H. van Esch**

Abstract: *Catalyst-assisted self-assembly is widespread in nature to achieve spatial control over structure formation. Reported herein is the formation of hydrogel micropatterns on catalytic surfaces. Gelator precursors react on catalytic sites to form building blocks which can self-assemble into nanofibers. The resulting structures preferentially grow where the catalyst is present. Not only is a first level of organization, allowing the construction of hydrogel micropatterns, achieved but a second level of organization is observed among fibers. Indeed, fibers grow with their main axis perpendicular to the substrate. This feature is directly linked to a unique mechanism of fiber formation for a synthetic system. Building blocks are added to fibers in a confined space at the solid–liquid interface.*

Herein we describe how control over the self-assembly of synthetic molecular fibers, using surface-confined catalysts, can lead to the formation of micropatterns of oriented supramolecular structures. Many vital processes in biological systems involve spatiotemporal control over directed self-assembly, for instance, regulation of active tension in muscles[1] or chromosome separation during cell division.[2] In these systems, spatiotemporal control of self-assembly has been achieved through enzymatic action[3] without intervention of external triggers. These in vivo processes have been reproduced with artificial systems using building blocks, such as actin monomers or GTP proteins,[4] found in cells or using biomolecules.[5] In contrast, spatiotemporal control over the formation of synthetic self-assembled systems is limited to stoichiometric triggers. Gradients of pH,[6] temperature,[7] concentration,[8] electric[9] or magnetic fields,[10] or the use of templates[11] or click-chemistry[12] have been used to control the formation of self-assembled structures in space. Various types of lithography are also used to create micropatterns of gels on surfaces, either by directly initiating growth of structures using photolithography[13] or by chemically modifying surfaces,[14] however the fibers composing these gels were not oriented structures. To this day, it remains a challenge to achieve directed self-assembly by catalytic action in fully synthetic systems.

For the work described herein, we use catalytic control over the rate of self-assembly to control the local formation of supramolecular gel fibers by employing a pattern of a catalyst immobilized on a surface. We find that the self-assembly process is confined to the catalytic sites at the substrate–liquid interface, and leads to a highly anisotropic fibrous network with a preferential orientation of the fibers perpendicular to the interface. Our results demonstrate the feasibility to control directed self-assembly in synthetic systems by the spatial confinement of catalytic activity. The resulting functional hydrogel micropatterns may be of particular interest in biology related research areas for in vitro studies on cells[15] or for sensing purposes.[16]

Recently, we designed a supramolecular hydrogelator system which enables control of the rate of self-assembly and the properties of the resulting materials through bulk catalysis.[17] The compound **3** (Figure 1 a) self-assembles in water to form fibers (see Figure S1 in the Supporting Information). Above a certain concentration threshold these fibers form networks which are capable of entrapping solvent, thus leading to hydrogels. The rate of formation of **3**, from cyclohexane-1,3,5-tricarbohydrazide (**1**) and three molecules of 3,4-bis[2-(2-methoxyethoxy)ethoxy]benzaldehyde (**2**), can be tuned in situ by acidic or nucleophilic catalysis.[18] Modulating the rate of formation of the building blocks **3** has a direct effect on the morphology and the mechanical properties of the resulting supramolecular structures.

On the basis these findings we anticipated that a surface-bounded catalyst should locally enhance the rate of formation of **3**, thus leading to fiber nucleation near the surface (Figure 1 b,i), as long as the self-assembly process is faster than diffusion. By localizing the catalysts in micrometer-scale patterns, a second level of spatial control over self-assembly can be exerted. In the current system, surface catalysis will lead to a surface-directed gradient in the concentration of **3** (Figure 1 b,ii). Thus, when the concentration of **3** surpasses the critical self-assembly concentration, fibers will start to grow.

For the present experiments sulfonic acid groups are used to catalyze hydrazone formation from **1** and **2**, thus leading to **3**. Surface-bound catalysis based on sulfonic acid functions is

[*] Dr. A. G. L. Olive, N. H. Abdullah, Dr. I. Ziemecka,[+] Dr. E. Mendes, Dr. R. Eelkema, Prof. Dr. J. H. van Esch
Advanced Soft Matter Group, Department of Chemical Engineering, Delft University of Technology
Julianalaan 136, 2628 BL Delft (The Netherlands)
r.eelkema @ tudelft.nl
j.h.vanesch @ tudelft.nl

[+] Current address: TIPs—Fluid Physics
Ecole Polytechnique de Bruxelles, ULB, CP165/67
avenue F.D. Roosevelt 50, 1050 Bruxelles (Belgium)

[**] Financial support from the Dutch Organisation for Scientific Research (NWO: ECHO and VIDI grants), the Ministry of Education Malaysia, and the University of Malaysia Kelantan is duly acknowledged. We are grateful to Jos Poolman for the preparation of compounds **1** and **2**, to Dr. Chandan Maity for the preparation of the fluorescent probe, as well as to Dr. L. C. P. M. de Smet and D. Ullien (TU Delft) for their help with XPS measurements.

Supporting information for this article is available on the WWW under http://dx.doi.org/10.1002/anie.201310776.

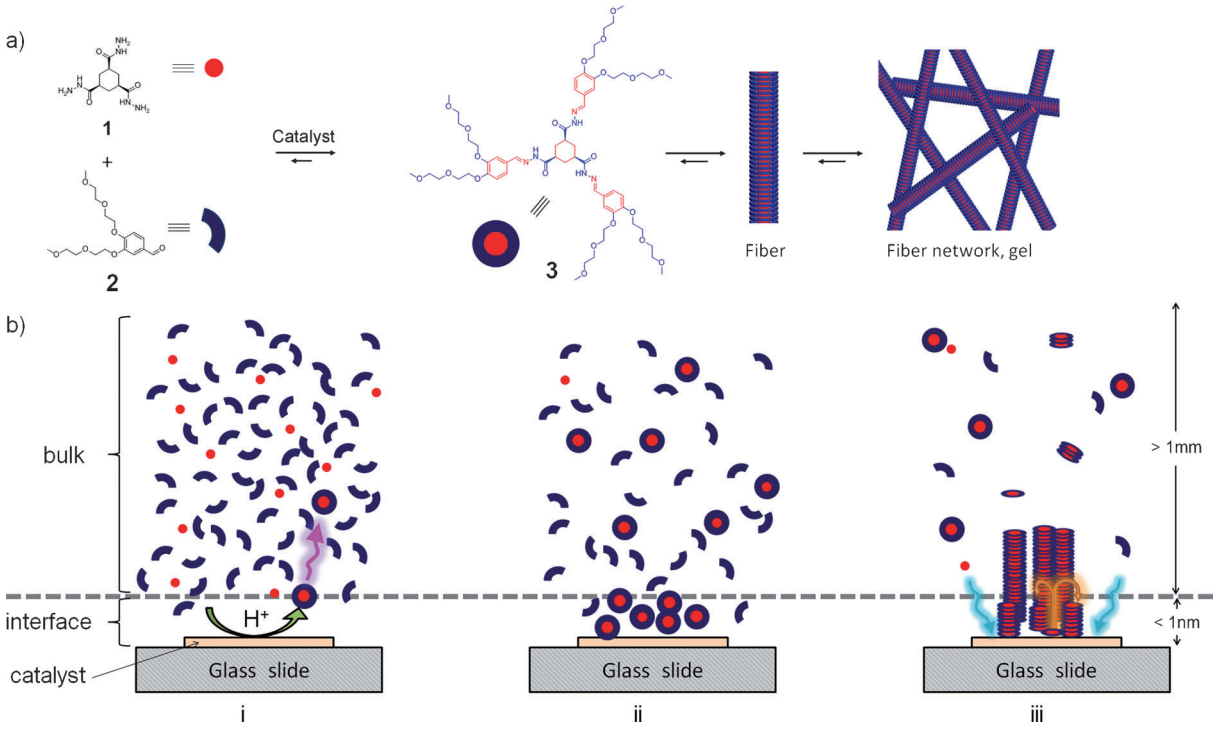

Figure 1. a) Illustration of the catalytic formation of the trishydrazone hydrogelator **3** from the soluble building blocks **1** and **2**, thus leading to fiber formation by self-assembly and subsequently to a network of fibers to trap the surrounding solvent to form a gel. b) Spatial control of directed self-assembly through a catalytic effect. i) formation of **3** in catalytic sites (green arrow) and its diffusion from the surface (purple arrow); ii) the higher density of **3** near the surface resulting from the fastest reaction rate; iii) the limited accessibility of the interface to **1** and **2** (blue arrows) and insertion of newly formed **3** at the top of the shortest fibers (orange arrows).

widely used for various chemical reactions, using mesoporous silica or polymeric fibers.[19] However, sulfonic acid groups with a pK_a value of 1.4[20] are expected to be fully dissociated within the optimal pH range of 3–5 for hydrazone formation. Therefore in our case, we relied on acidic catalysis caused by an increased proton concentration near negatively charged sulfonate surfaces, rather than specific acid catalysis by the sulfonic acid moieties.

Patterned sulfonic acid catalyst surfaces were prepared by soft-lithography.[21] First, a thiol pattern was covalently attached to a glass surface by microcontact printing.[21] Next, the desired sulfonic acid patterns were obtained by oxidation of the thiol groups using hydrogen peroxide (see part C of the Supporting Information).

The catalyst-patterned glass slides were then brought into contact with a solution containing the precursors **1** and **2**, and the fibers started to grow on the catalyst patterns. In a typical experiment, a poly(dimethylsiloxane) (PDMS) cuvette containing **1** and **2** in a 1:6 ratio (2 aldehyde groups per acylhydrazide group) at a concentration of 20 mM of **1** in a phosphate buffer was carefully placed on the catalyst-patterned glass (see Figures S4 and S5). To follow the self-assembly of **3** by confocal fluorescence microscopy, a fluorescence probe carrying an aldehyde function was added at a concentration of 0.02 mM (see Figure S6). Also, this probe reacts with **1** and is incorporated within the fibers, thus enabling imaging of the structures.[17] At both bulk pH values of 5 and 7 we observed that fibers started to grow from the surface areas covered with sulfonate groups, and within 5–60 minutes, depending on the pH value, hydrogel patterns formed with a maximum height of 5.5 micrometers. Interestingly, the maximum attained height of the patterns depends on the concentration of **1** and **2**, but does not depend on the pH value. Over much longer times, fiber formation was also observed in the bulk solution. Interestingly, in between "surface" fibers and "bulk" fibers, a 10 to 20 micrometer wide depletion zone is observed. In this area, no self-assembled structures were present, thus suggesting different kinetics for the formation of fibers and that the growth of fibers might be limited by diffusion. A variety of shapes and dimensions were examined, including lines, circles, squares, and rectangles, (Figure 2) having dimensions ranging from 10 to 100 micrometers, and in all cases the hydrogel patterns closely follow the catalyst pattern underneath. Nucleation and fiber growth can be influenced by the nature of the chemical functions on the surface. It should be noted that control experiments performed using a pattern displaying thiol functions did not lead to preferential growth, thus indicating that neutral (3-mercaptopropyl)trimethoxysilane (MPTS) monolayers, without acid functionalities, do not affect self-assembly by either catalysis or affinity. In this case, randomly scattered fibers on the surface were observed. These results clearly indicate that fiber formation is induced by the surface-confined sulfonate groups.

To further corroborate the catalytic effect of interfacial pH values on the hydrazone formation leading to local fiber formation, we investigated the influence of the pH value on gel-pattern formation in more detail. First, imaging an edge of

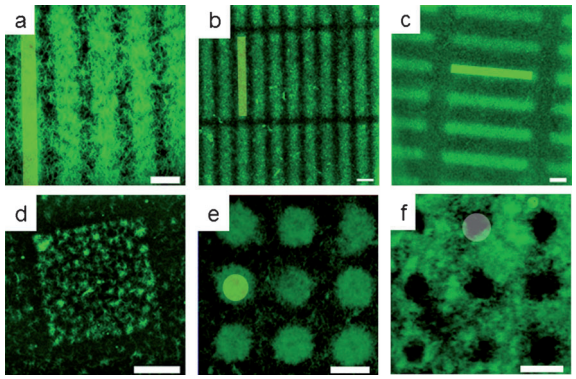

Figure 2. Confocal microscopy images of patterns, composed of self-assembled fibers of **3**, which reflect the previously stamped catalytic pattern shown by the yellow areas on the images. a) Lines: 10 μm width with 15 μm spacing, b) rectangle: 10×100 μm with 10 μm spacing, c) 10×100 μm rectangles with 25 μm spacing, d) square of 50×50 μm, e) discs with 15 μm diameter and 20 μm spacing f) negative image of (e). Scale bars: 20 μm).

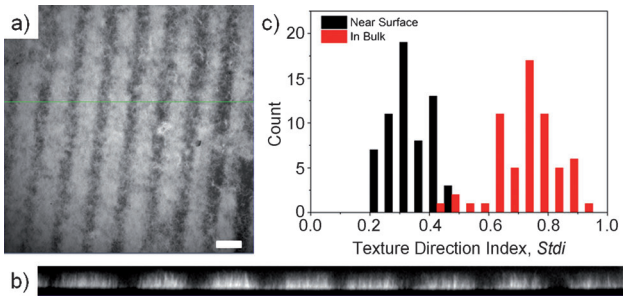

Figure 3. Confocal microscopy images of line patterns, composed of self-assembled fibers of **3**, which reflect the previously stamped catalytic pattern (lines with 10 μm width and 15 μm spacing). a) The *xy* plane; b) *xz* plane corresponding to the green line on image (a). c) Texture direction index distribution from fibers in bulk (red) and near the surface (black).

the stamped area (see Figure S8) showed that fibers not only grow preferentially where the catalyst is present, but also that near the surface their density is much higher than in bulk. Fibers fully cover the surface where sulfonic acids are present, whereas they are scattered on native glass, thus showing that the concentration of **3** in catalytic areas is higher at all times as compared to noncatalytic surfaces. In bulk, the kinetics of the formation of **3** depend strongly on the pH values and was found to be two orders of magnitude faster at pH 5 than at pH 7.[17,22] On patterned surfaces immersed in solutions of pH 5 and pH 7, the first fibers appeared after 5 and 60 minutes on the catalyst patterns, respectively. Whereas at pH 5 the fiber formation was completed 2–3 minutes later, it took another hour at pH 7, after the formation of the first fibers, to complete the reaction (see movies in the Supporting Information). Simulation of the system in 0.1M sodium phosphate buffer using the Grahame equation showed that the interfacial pH value is decreased by approximately 1.5 pH units compared to the bulk pH value (see the Supporting Information). Hence, the above experiments at a bulk pH value of 5 and 7 correspond to an approximate interfacial pH value of 3.5 and 5.5, and the time scales of fiber formation at these interfacial pH values nicely match the time scales of fiber formation at a bulk pH value of 3–5 as observed previously. Interestingly, fiber formation is two orders of magnitude slower in bulk at pH 7. To achieve an interfacial pH value at the catalytic patterns of around 7, the pH of the buffer has to be raised to 9. Indeed, when using a pH 9 buffered solution on a catalytic surface, no pattern formation resulting from self-assembly was observed after 5 hours. At a bulk pH value of 9, the concentration of protons near the catalytic surface is too low to achieve a reasonable reaction rate. These simulations also showed that increased proton concentration is confined to a 5 nm layer at the interface. These results unambiguously show that interfacial acid catalysis is required for the formation of surface-confined patterns of self-assembled fibers.

To gain further insight into the mechanism of fiber and gel formation we studied the interfacial network in more detail. Interestingly, careful imaging and analysis of the fiber network structure near the catalytic surface revealed directionality in the fiber orientation. From visual inspection of the cross-sectional micrograph (Figure 3b) obtained from three-dimensional imaging of line patterns (Figure 3a), the fibers within the surface patterns appear to be aligned and oriented perpendicular to the substrate. We analyzed the fiber alignment using an empirical parameter, the texture direction index S for fibers in bulk and for fibers near the surface (see part F of the Supporting Information for procedure). Theoretically, S ranges from 0 (perfect parallel alignment) to 1 (completely isotropic).[23] Indeed, fibers within the surface pattern had an S index of 0.30 ± 0.10 whereas fibers in bulk had $S = 0.75 \pm 0.10$ (Figure 3c), thus showing that fibers near the surface have a preferential orientation perpendicular to the solid substrate, whereas gel patches in the bulk consist of randomly oriented fibers (see Figure S9). Simulations using the Grahame equation show that the acidic electrostatic double layer near the surface is not larger than 1 nm, therefore orientation which occurs over a 5.5 micrometer distance cannot be attributed to proton gradients. This result shows that fibers near the surface are formed through a different mechanism than that for the bulk fibers; if it were merely bulk fibers sticking to the surface they should have similar (isotropic) S factors as observed on noncatalytic patterns such as thiols.

Our results explicitly show that the formation of interfacial fibrous gel patterns is due to the local formation of **3** by interfacial acid catalysis. This situation poses an interesting question with regard to how and where the locally formed hydrogelator molecules add to the growing fibers. Two situations can be envisioned: 1) new hydrogelator molecules are inserted into the growing fibers in between the fiber tip and substrate, because of the high local concentration of hydrogelator, or 2) new hydrogelator molecules diffuse away from the interface and add to the growing fiber tips at the bulk side, because of steric reasons. To test these two hypotheses, we investigated the fiber-growth mechanism by bleaching the fluorescence of part of the growing fibers on the catalytic

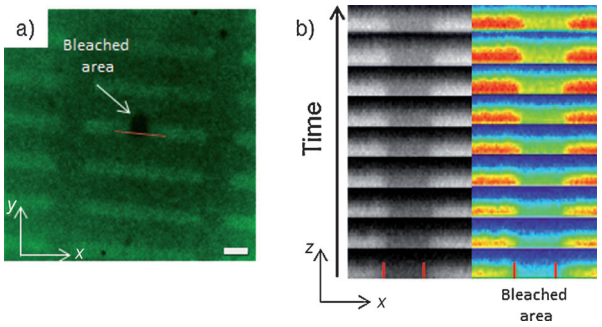

Figure 4. Confocal microscopy images of fibers grown on rectangular pattern. a) A bleached area in the *xy* plane; scale bar: 20 μm. b) The *xz* plane as a function of time. Images were taken every 5 min.

surface (Figure 4a). By recording three-dimensional images of the bleached area as a function of time, the recovery of emission resulting from the insertion of new building blocks is monitored. In the nonbleached area, fibers are still growing as seen in Figure 4b, where the height of gel increases from 1 to 3 micrometers over the course of the experiment. Meanwhile, the emission becomes more and more intense as a function of time, thus showing that even if fibers are already present their density increases, either because fibers branch, become thicker in time, or new fibers nucleate at the interface. For the bleached area, initially we observe an increase of emission near the substrate, which with time progresses towards the fiber-bulk interface (Figure 4b). However, the overall fluorescence intensity remains lower than the unbleached areas at every distance from the surface.

These experiments clearly show that the insertion of new hydrogelator molecules preferentially occurs near the catalytic surface. However, instead of inserting in between the substrate and a growing fiber, the observations rather point to a growth mechanism in which newly formed hydrogelator molecules add to the already present fibers leading to branching, thickening, or nucleation of new fibers. Moreover, these experiments also show that above a certain quantity of fibers formed, the catalytic surface is no longer accessible, thereby effectively stopping fiber growth and limiting the thickness of the gel surface pattern.

The above mechanism explains how the interface becomes less accessible in time to **1** and **2**. In fact, this limited approachability may also be at the origin of the orientation and directionality in growth of the fibers. It may be that when the first structures are formed above the catalytic pattern, the latter is no longer accessible from the top for **1** and **2**. The flow of reactants is created on the edges of the catalytic pattern through conversion and depletion, thus inducing alignment of the forming fibrous structures.

In conclusion, we have demonstrated that it is possible to grow patterns of oriented self-assembled fibers using patterned catalytic surfaces. By locally changing the reaction rate between two precursor molecules using a surface-bound catalyst, fiber building blocks are generated near the surface and lead to localized fiber growth. Confining the catalyst in patterns results in the formation of patterned, out-of-equilibrium gel materials. The mechanism of action of this fully synthetic system is reminiscent of that of filaments found in the cycloskeleton.[24] We believe that this system can serve as a starting point for fundamental studies regarding directional forces generated by self-assembly. Because of the the ease of fiber functionalization using dynamic covalent chemistry, and the possibility to tune both stiffness and local density (patterning), this system may find application in mechanobiology to study cell adhesion, spreading, and differentiation.[25]

Received: December 12, 2013
Published online: March 11, 2014

Keywords: interfaces · micropatterns · nanostructures · self-assembly · surface chemistry

[1] J. M. Barral, H. F. Epstein, *BioEssays* **1999**, *21*, 813–823.
[2] R. Li, D. F. Albertini, *Nat. Rev. Mol. Cell Biol.* **2013**, *14*, 141–152.
[3] Y. Gao, C. Berciu, Y. Kuang, J. Shi, D. Nicastro, B. Xu, *Acs Nano* **2013**, *7*, 9055–9063.
[4] a) A. C. Reymann, J. L. Martiel, T. Cambier, L. Blanchoin, R. Boujemaa-Paterski, M. Thery, *Nat. Mater.* **2010**, *9*, 827–832; b) R. Galland, P. Leduc, C. Guerin, D. Peyrade, L. Blanchoin, M. Thery, *Nat. Mater.* **2013**, *12*, 416–421; c) C. Hoffmann, E. Mazari, S. Lallet, R. Le Borgne, V. Marchi, C. Gosse, Z. Gueroui, *Nat. Nanotechnol.* **2013**, *8*, 199–205.
[5] a) A. R. Hirst, S. Roy, M. Arora, A. K. Das, N. Hodson, P. Murray, S. Marshall, N. Javid, J. Sefcik, J. Boekhoven, J. H. van Esch, S. Santabarbara, N. T. Hunt, R. V. Ulijn, *Nat. Chem.* **2010**, *2*, 1089–1094; b) J. D. Hartgerink, E. Beniash, S. I. Stupp, *Science* **2001**, *294*, 1684–1688.
[6] I. Ziemecka, G. J. M. Koper, A. G. L. Olive, J. H. van Esch, *Soft Matter* **2013**, *9*, 1556–1561.
[7] M. P. Valignat, O. Theodoly, J. C. Crocker, W. B. Russel, P. M. Chaikin, *Proc. Natl. Acad. Sci. USA* **2005**, *102*, 4225–4229.
[8] R. M. Capito, H. S. Azevedo, Y. S. Velichko, A. Mata, S. I. Stupp, *Science* **2008**, *319*, 1812–1816.
[9] A. Winkleman, B. D. Gates, L. S. McCarty, G. M. Whitesides, *Adv. Mater.* **2005**, *17*, 1507–1511.
[10] I. O. Shklyarevskiy, P. Jonkheijm, P. C. M. Christianen, A. P. H. J. Schenning, A. Del Guerzo, J. P. Desvergne, E. W. Meijer, J. C. Maan, *Langmuir* **2005**, *21*, 2108–2112.
[11] E. D. Sone, E. R. Zubarev, S. I. Stupp, *Angew. Chem.* **2002**, *114*, 1781–1785; *Angew. Chem. Int. Ed.* **2002**, *41*, 1705–1709.
[12] G. Y. Qing, H. Xiong, F. Seela, T. L. Sun, *J. Am. Chem. Soc.* **2010**, *132*, 15228–15232.
[13] A. Revzin, R. J. Russell, V. K. Yadavalli, W.-G. Koh, C. Deister, D. D. Hile, M. B. Mellott, M. V. Pishko, *Langmuir* **2001**, *17*, 5440–5447.
[14] W. Lee, D. Choi, Y. Lee, D.-N. Kim, J. Park, W.-G. Koh, *Sens. Actuators B* **2008**, *129*, 841–849.
[15] a) C. S. Chen, M. Mrksich, S. Huang, G. M. Whitesides, D. E. Ingber, *Science* **1997**, *276*, 1425–1428; b) H. Komatsu, S. Tsukiji, M. Ikeda, I. Hamachi, *Chem. Asian J.* **2011**, *6*, 2368–2375.
[16] T. H. Park, M. L. Shuler, *Biotechnol. Prog.* **2003**, *19*, 243–253.
[17] J. Boekhoven, J. M. Poolman, C. Maity, F. Li, L. van der Mee, C. B. Minkenberg, E. Mendes, J. H. van Esch, R. Eelkema, *Nat. Chem.* **2013**, *5*, 433–437.
[18] a) V. T. Bhat, A. M. Caniard, T. Luksch, R. Brenk, D. J. Campopiano, M. F. Greaney, *Nat. Chem.* **2010**, *2*, 490–497; b) A. Dirksen, S. Dirksen, T. M. Hackeng, P. E. Dawson, *J. Am. Chem. Soc.* **2006**, *128*, 15602–15603.
[19] A. El Kadib, A. Finiels, D. Brunel, *Chem. Commun.* **2013**, *49*, 9073–9076.

[20] I. K. Mbaraka, B. H. Shanks, *J. Catal.* **2006**, *244*, 78 – 85.
[21] a) Y. N. Xia, X. M. Zhao, G. M. Whitesides, *Microelectron. Eng.* **1996**, *32*, 255 – 268; b) J. L. Wilbur, A. Kumar, E. Kim, G. M. Whitesides, *Adv. Mater.* **1994**, *6*, 600 – 604.
[22] J. M. Poolman, J. Boekhoven, A. Besselink, A. G. L. Olive, J. H. van Esch, R. Eelkema, *Nat. protoc.* **2014**, DOI: 10.1038/nprot.2014.055.
[23] I. M. Scanning Probe Image Processor (SPIP) Version 2.000, A/S, Lyngby, Denmark.
[24] B. Alberts, A. Johnson, J. Lewis, M. Raff, K. Roberts, P. Walter in *Molecular Biology of the Cell*, 4th ed. (Ed.: G. Science), New York, **2002**.
[25] J. Boekhoven, C. M. Rubert Pérez, S. Sur, A. Worthy, S. I. Stupp, *Angew. Chem.* **2013**, *125*, 12299 – 12302; *Angew. Chem. Int. Ed.* **2013**, *52*, 12077 – 12080.